SSS-TR-93-13915

NUMERICAL MODELS OF QUARRY BLAST SOURCES: THE EFFECTS OF THE BENCH

T. G. Barker
K. L. McLaughlin
J. L. Stevens
S. M. Day

Maxwell Laboratories, Inc.
S-CUBED Division
P.O. Box 1620
La Jolla, CA 92038-1620

May 1993

Semiannual Report

Phillips Laboratory
Kirtland Air Force Base, NM 87117-5320

REPORT DOCUMENTATION PAGE

Form Approved
OMB No. 0704-0188

1. AGENCY USE ONLY *(Leave blank)*	2. REPORT DATE	3. REPORT TYPE AND DATES COVERED
	1 May 1993	Technical Report 11/1/92-4/15/93

4. TITLE AND SUBTITLE
NUMERICAL MODELS OF QUARRY BLAST SOURCES: THE EFFECTS OF THE BENCH

5. FUNDING NUMBERS
F29601-91-C-DB27

6. AUTHOR(S)
T. G. Barker, K. L. McLaughlin, J. L. Stevens and S. M. Day

7. PERFORMING ORGANIZATION NAME(S) AND ADDRESS(ES)
Maxwell S-CUBED Division
P.O. Box 1620
La Jolla, CA 92038-1620

8. PERFORMING ORGANIZATION REPORT NUMBER
SSS-TR-93-13915

9. SPONSORING/MONITORING AGENCY NAME(S) AND ADDRESS(ES)
DARPA-NMRO
3701 N. Fairfax Dr. #717
Arlington, VA 2203-1714

Phillips Laboratory (PL/PKVA)
3651 Lowry Avenue, SE
Kirtland, AFB, NM 87117-5777

10. SPONSORING/MONITORING AGENCY REPORT NUMBER

11. SUPPLEMENTARY NOTES

12a. DISTRIBUTION/AVAILABILITY STATEMENT
Approved for Public Release; Distribution Unlimited

12b. DISTRIBUTION CODE

13. ABSTRACT *(Maximum 200 words)*

A set of finite difference calculations were performed to model the effects of a quarr bench on the excitation of seismic signals from a quarry. This work complements othe S-CUBED research on the nonlinear behavior of the quarry blast source (spall from th quarry face) and interference effects from ripple-fired explosions. We find that th excitation of seismic phases depends strongly on the location of the explosion source nea the quarry face. In particular, we find that:

1. Seismic signals from point explosion (dilatational) sources located behind the quarr face can be reduced substantially in amplitude, while seismic waves from sources on th quarry floor may be amplified. The source amplitude variations occur for sources withi about one bench height of the quarry face. The numerical simulations presented in thi study can be used to estimate and correct for this effect.
2. An extended source in the standard configuration (charges placed a distance of 1/2 th bench height from the quarry face and extending to the depth of the quarry floor) averages

14. SUBJECT TERMS
Nuclear Discrimination
Synthetic Seismograms
Quarry Blast
Nuclear Testing

15. NUMBER OF PAGES

16. PRICE CODE

17. SECURITY CLASSIFICATION OF REPORT	18. SECURITY CLASSIFICATION OF THIS PAGE	19. SECURITY CLASSIFICATION OF ABSTRACT	20. LIMITATION OF ABSTRAC
UNCLASSIFIED	UNCLASSIFIED	UNCLASSIFIED	

CLASSIFIED BY:

DECLASSIFY ON:

13. Abstract *(Continued)*

2. these variations leading to a source that is reduced slightly in amplitude relative to a source in a half space.
3. The amplitude variations occur because a dilatational source such as an explosion is strongly affected by the presence of a free surface close to the source. Seismic signals from point forces are affected very little by proximity to the quarry face.
4. These results are nearly independent of the takeoff angle of the seismic signal.
5. Rayleigh wave amplitudes are reduced by up to 40 percent.

Table of Contents

Section		Page
Summary		vi
1	Introduction	1
2	Numerical Simulations of Explosions Near a Quarry Bench	2
2.1	Methodology	2
2.2	Results of Simulations	2
2.2.1	Body Waves	7
2.2.1	Rayleigh Waves	14
3	Discussion	25
4	Conclusions	29
5	References	31

List of Illustrations

Figure		Page
1	Schematic drawing of a row of charges at the face of a quarry blast	3
2	Schematic drawing of the reciprocal theorems used in this report	4
3	Schematic drawing of the numerical simulations, showing incident body and Rayleigh waves on a free surface with a step	6
4	Locations on numerical grid at which displacements, dilatations and rotations from incident body waves were saved for analysis	8
5	Vertical displacements due to a P wave incident at 30° from the vertical low pass filtered with corner at 15 Hz	9
6	Dilatations due to a P wave incident at 30° from the vertical, low pass filtered with corner at 15 Hz	10
7	Exploded view of the bench from Figure 6: Dilatations due to a P wave incident at 30° from the vertical, low pass filtered with corner at 15 Hz	11
8	Dilatations due to a P wave incident at 60° from the vertical, low pass filtered with corner at 15 Hz. The dimensions of the plot are 140 m x 50 m	12
9	Exploded view of the bench showing dilatations due to a P wave incident at 30° from the vertical, low pass filtered with corner at 10 Hz. The dimensions of the plot are 100 m x 50 m	13
10	Exploded view of the bench showing dilatations due to a P wave incident at 30° from the vertical, low pass filtered with corner at 15 Hz (step down). The dimensions of the plot are 100 m x 50 m	15
11	Exploded view of the bench showing dilatations due to an SV wave incident at 30° from the vertical, low pass filtered with corner at 15 Hz	16
12	Exploded view of the bench showing rotations due to a P wave incident at 30° from the vertical, low pass filtered with corner at 15 Hz	17
13	Rotations due to a SV wave incident at 30° from the vertical, low pass filtered with corner at 15 Hz	18

List of Illustrations (Continued)

Figure		Page
14	Normalized dilatation field for Rayleigh waves experiencing a step up in topography, low pass filtered with corner at 15 Hz	19
15	Normalized dilatation field for Rayleigh waves experiencing a step down in topography, low pass filtered with corner at 15 Hz	20
16	Locations on numerical grid at which displacements, dilatations and rotations from incident Rayleigh waves were saved for analysis (top) step up and (bottom) step down	21
17	Normalized displacement field for Rayleigh waves experiencing a step up in topography, low pass filtered with corner at 15 Hz	23
18	Normalized displacement field for Rayleigh waves experiencing a step down in topography, low pass filtered with corner at 15 Hz	24
19	Bench geometry	26

Summary

A set of finite difference calculations were performed to model the effects of a quarry bench on the excitation of seismic signals from a quarry. This work complements other S-CUBED research on the nonlinear behavior of the quarry blast source (spall from the quarry face) and interference effects from ripple-fired explosions. We find that the excitation of seismic phases depend strongly on the location of the explosion source near the quarry face. In particular, we find that:

1. Seismic signals from point explosion (dilatational) sources located behind the quarry face can be reduced substantially in amplitude, while seismic waves from sources on the quarry floor may be amplified. The source amplitude variations occur for sources within about one bench height of the quarry face. The numerical simulations presented in this study can be used to estimate and correct for this effect.

2. An extended source in the standard configuration (charges placed a distance of 1/2 the bench height from the quarry face and extending to the depth of the quarry floor) averages these variations leading to a source that is reduced slightly in amplitude relative to a source in a half space.

3. The amplitude variations occur because a dilatational source such as an explosion is strongly affected by the presence of a free surface close to the source. Seismic signals from point forces are affected very little by proximity to the quarry face.

4. These results are nearly independent of the takeoff angle of the seismic signal.

5. Rayleigh wave amplitudes are reduced by up to 40 percent.

1. Introduction

In our recent annual report (Barker, *et al.* 1993), we modeled several important aspects of the quarry blast source including horizontal and vertical spall from the quarry blast face and the effect of superposition of ripple-fired explosions. We also examined the effectiveness of a large quarry blast source for hiding a clandestine nuclear test. In this report, we examine the effect of the location of the source within the quarry. Stevens, *et al.* (1993), found that surface waves from underground nuclear explosions could be reduced substantially in amplitude by the presence of a vertical boundary close to the explosion. This brings up the question of how the quarry face affects the seismic signal from the quarry blast, whether it causes any of the seismic signals from the quarry blast to be amplified or reduced in amplitude, and whether it leads to any characteristics of the seismic signals that could be used to identify the source as a quarry blast.

To answer these questions, we have performed a series of finite difference calculations for an explosion located at a suite of locations near a quarry bench. We also perform a theoretical analysis and find an analytic solution to this problem valid for wavelengths much larger than the height of the quarry face, which includes nearly all seismic signals of interest.

2. Numerical Simulations of Explosions Near a Quarry Bench

2.1 Methodology

An explosive charge in a standard configuration for a quarry blast is shown in Figure 1. The seismic signals from this source result from a linear component, the signals due to a dilatational source in this structure; and a nonlinear component, the nonlinear motion (spall and ballistic motion) of the material broken from the quarry face. To calculate the linear component to the quarry blast source, we use the approach described by McLaughlin and Jih (1988), using the elastic reciprocity theorem (e.g. Aki and Richards, 1980) to find the far-field displacements due to a point explosive source by calculating the dilatation at the desired source point caused by an incident plane wave (see Figure 2).

This reciprocal approach has several advantages over the conceptually more direct approach, which would be to locate explosive and force sources at source locations near the bench and compute the resulting far-field wavefields. The first advantage is that the reciprocal approach yields the far-field wavefield. In order to find the far-field signals from the direct approach, one must either use a numerical grid sufficiently large to propagate the signals several wavelengths to the far field or devise a continuation scheme similar to the one used in numerous S-CUBED reports to find the far-field waves from nonlinear sources (e.g., Barker and Day, 1990). For 5 Hz signals in a material with a P wave velocity of 5000 m/sec, the wavelength is 1000 meters, so the grid would need to be at least several km in each direction to reach the far field and several more km to minimize interference from boundary reflections. Adequate description of the topographic bench requires a grid spacing less than 5 meters and the resulting grid would be quite large. A continuation scheme would require far-field propagation Green's functions for a medium with a bench on the free surface, for which there currently are no analytic solutions. Another advantage of the reciprocal approach is that one calculation yields the excitation for many source locations in and near the bench (at each grid point).

McLaughlin and Jih (1988) show that, if $U(\tau,\hat{s})$ is the displacement in the very far-field due to a point explosive source along the direction $\hat{s}$ at delayed

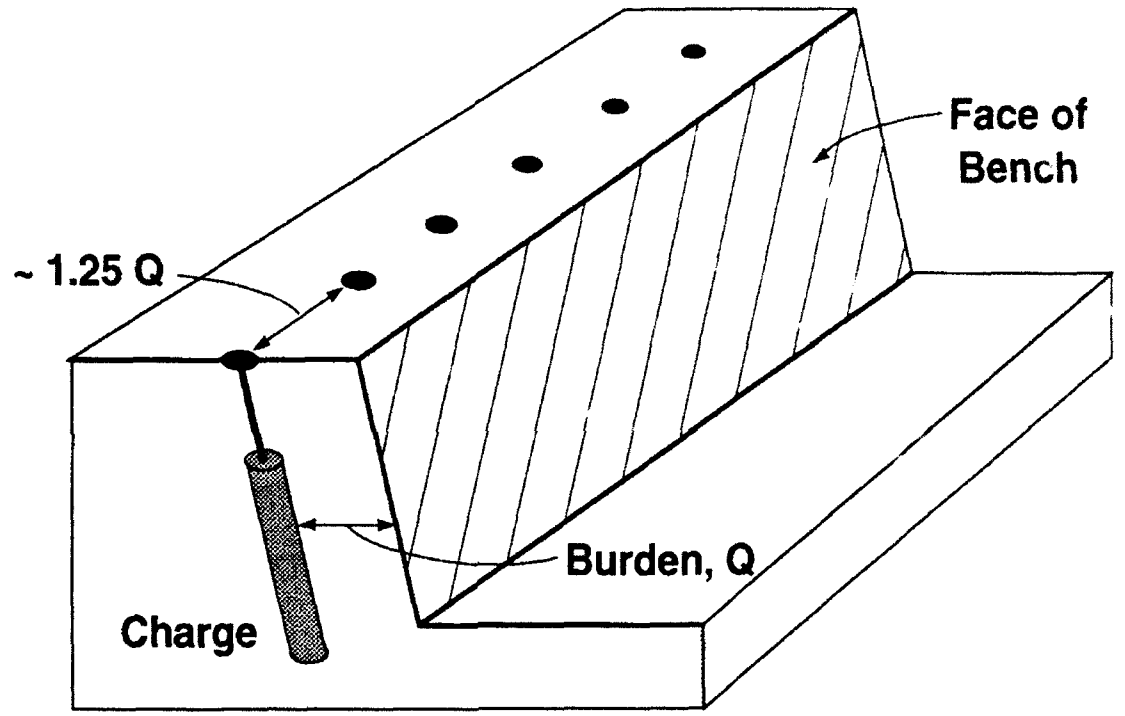

Figure 1. Schematic drawing of a row of charges at the face of a quarry blast.

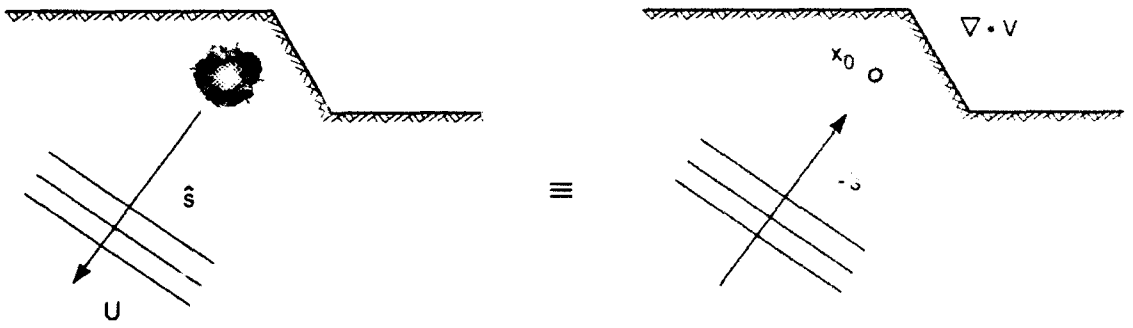

Figure 2. Schematic drawing of the reciprocal theorems used in this report.

time τ, and if $v(x_o, \tau)$ is the velocity due to a plane wave incident at x_o from infinity, then

$$U(\tau, \hat{s}) = C \nabla \cdot v(x_o, \tau), \tag{1}$$

where C is a constant of proportionality. Note that the reciprocal theorem states the equivalence between point force sources and displacements in the same direction so that by saving displacements as well as the dilatations, we can also deduce the response due to point forces in the bench. A similar approach is used by Okamoto (1993). The finite difference methods, in particular those for treating the free surface topography, are discussed in Jih, *et al* (1988) and McLaughlin and Jih (1988).

We have performed two-dimensional finite difference calculations for incident plane P and SV waves at several angles of incidence as well as for Rayleigh waves incident upon the bench from up-slope and down-slope, as shown in Figure 3. The numerical grid is 400 meters in the horizontal direction (with the bench at the center) and 200 meters in the vertical direction, with a uniform grid spacing of 2 meters. The calculations were run at 500 time steps per second for 1001 cycles (duration of 0.2 seconds). The bench height is 18 meters and slopes at 45°, approximated by 9 steps of 2 meters. The calculations are valid to about 20 Hz, above which numerical dispersion corrupts the results. The high sample rate was dictated by the small grid dimension required to define the bench. For the body wave calculations, wave motion was initiated from the right side of the grid along a line inclined normal to the incidence angle passing through a point 600 meters from the free surface in the center of the grid. The wave shape is that if an Ohnaka pulse. The Rayleigh wave calculations were initiated 500 meters to the left of the bench. The initial motions had the spatial and temporal properties of a Rayleigh wave convolved with a Ricker wavelet (Sheriff and Geldart, 1982). In addition to the calculations with the bench, we made comparable calculations with a flat surface, as references. By comparing the reference calculations to analytic solutions, we verified the usable bandwidth of the suite of calculations. Then by comparing the reference calculations with those including the bench, we isolated the effects of the bench.

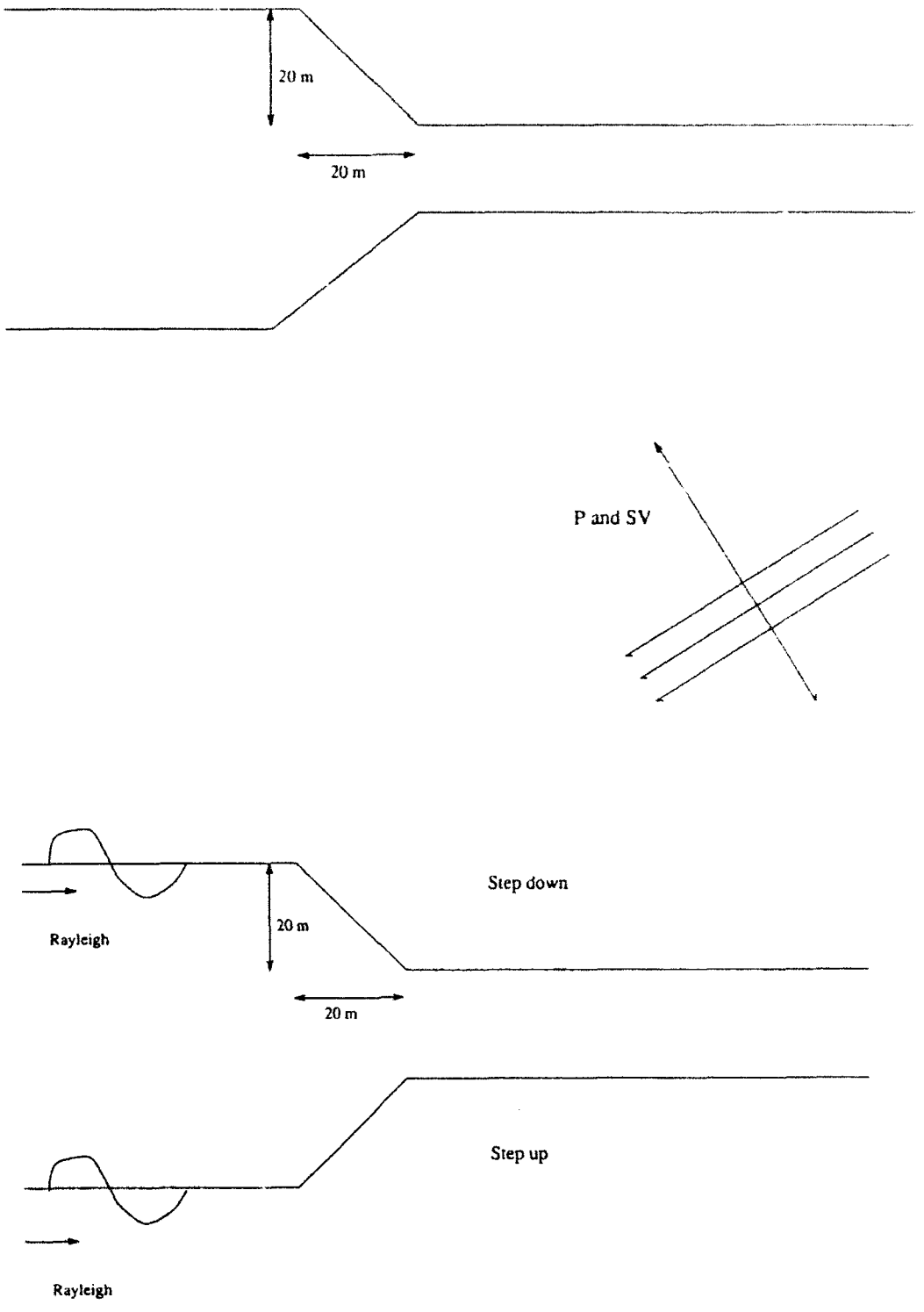

Figure 3. Schematic drawing of the numerical simulations, showing incident body and Rayleigh waves on a free surface with a step.

2.2. Results of Simulations

2.2.1 Body Waves

At the locations shown in Figure 4, we monitored vertical and horizontal displacement, dilatation and shear strain due to incident P and SV waves. We show in Figures 5 and 6 the vertical displacements and dilatations, respectively, due to a P wave incident at 30° from the vertical traveling right to left. The amplitudes, indicated by both contour lines and grayscale intensity, are normalized to the amplitudes from a reference calculation with a flat surface and the same incident P wave. The reference amplitude at a grid location is the amplitude at the same distance below the free surface as the location. Thus, using the reciprocity arguments presented above, the amplitudes can be viewed as the excitation at each grid point, relative to the excitation in a half space. The signals have been low-pass filtered using an 8-pole Butterworth filter whose corner frequency is 15 Hz. As can be seen from Figure 5, the vertical displacements deviate very little from 1.0 across the grid. The dilatations show much greater variability, especially near the bench. Figure 7 zooms in on the bench, where it can be seen that amplitudes are reduced by as much as a factor of 5 on the bench, and increased by a factor of 3 directly in front of the bench. Since quarry blasting takes place behind the bench at a horizontal distance comparable to the height of the bench (Figure 1), the effect of the bench is to reduce the excitation of waves from the explosive charges (the dilatational sources) by about a factor of two for waves traveling to the right (in the sense in Figures 6 and 7). However, the signals caused by movement of spall mass, represented by vertical and horizontal forces, are effected very little by the bench, as evidenced by the small variation in displacement seen in Figure 5. In Figure 8, we show the dilatation field for a P wave incident at 60° from vertical. The results are similar to those in Figure 6, where the incidence angle is 30°, indicating that the excitation is not sensitive to take-off angle. The dilatation field for a different corner frequency, 10 Hz, and for a take-off angle of 30° are shown in Figure 9. Comparison with Figure 7 shows that in the bandwidth of these calculations, the conclusions are not dependent on frequency.

Note that in Figures 5 through 8 there is an amplification directly in front of the bench. Apparently, the bench concentrates compressive stresses at the foot of

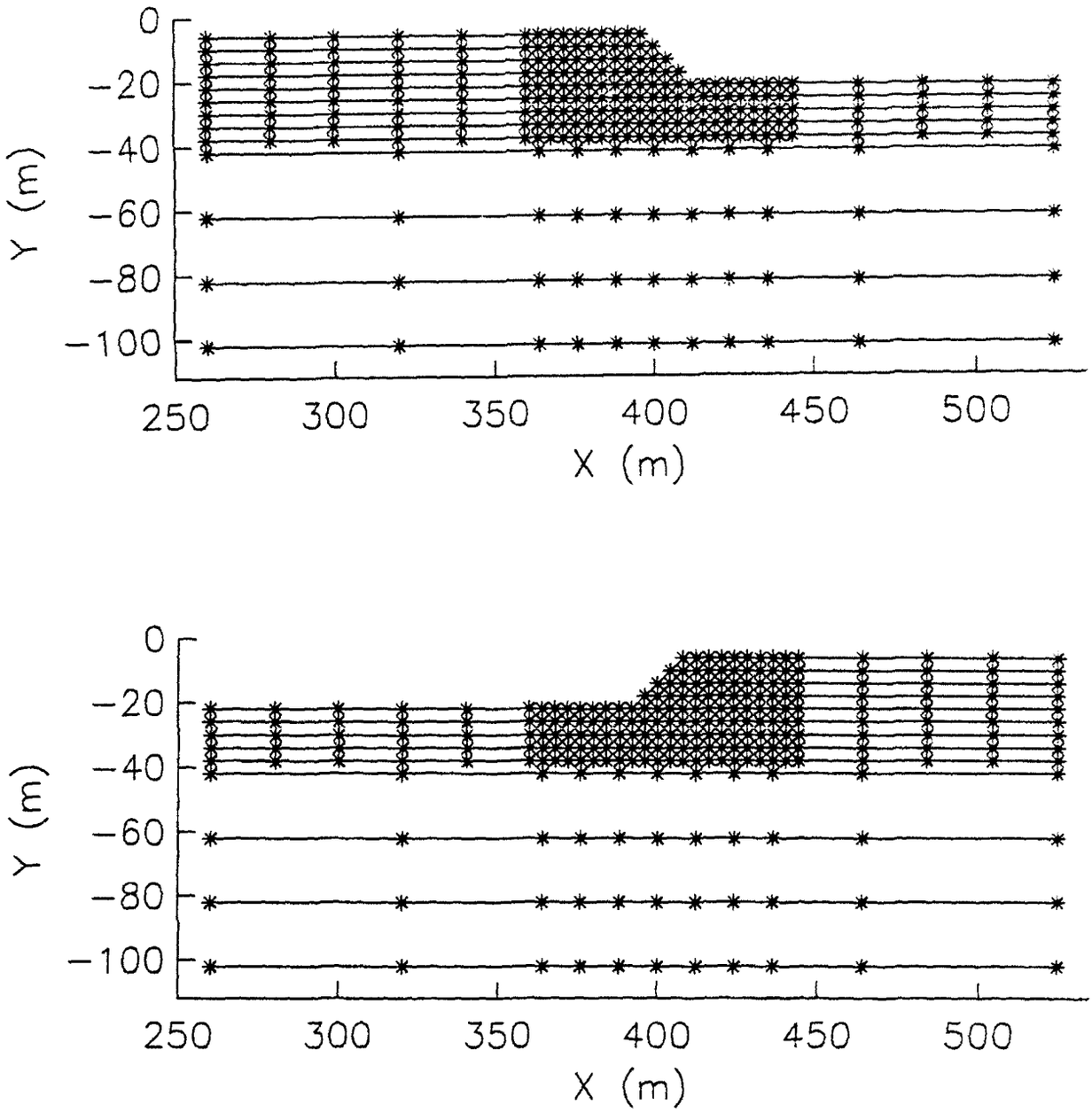

Figure 4. Locations on numerical grid at which displacements, dilatations and rotations from incident body waves were saved for analysis. Waves are incident from the lower right. (Top) step up, (bottom) step down.

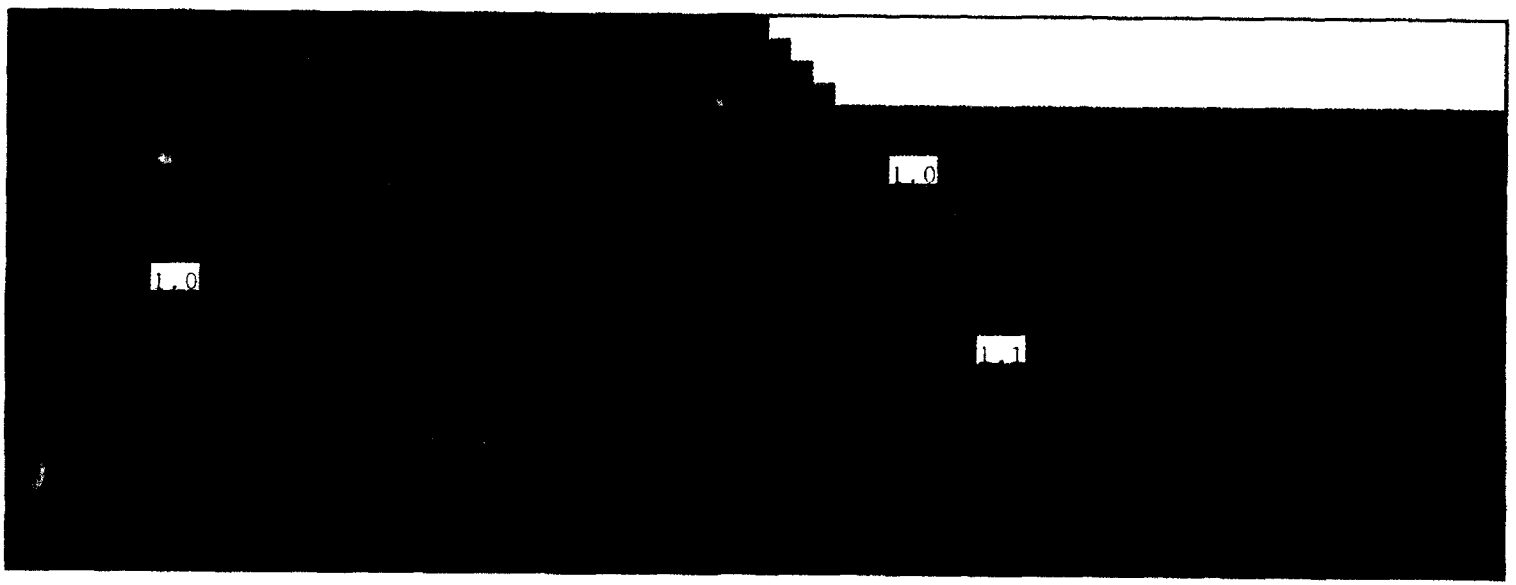

Figure 5. Vertical displacements due to a P wave incident at 30° from the vertical low pass filtered with corner at 15 Hz. The dimensions of the plot are 290 m x 110 m. The amplitudes, indicated by both contour lines and grayscale intensity, are normalized to the amplitudes from a reference calculation with a flat surface and the same incident P wave. The reference amplitudes at a grid location is the amplitude at the same distance below the free surface as the location. The amplitudes can be viewed as the excitation by a vertical force at each grid point.

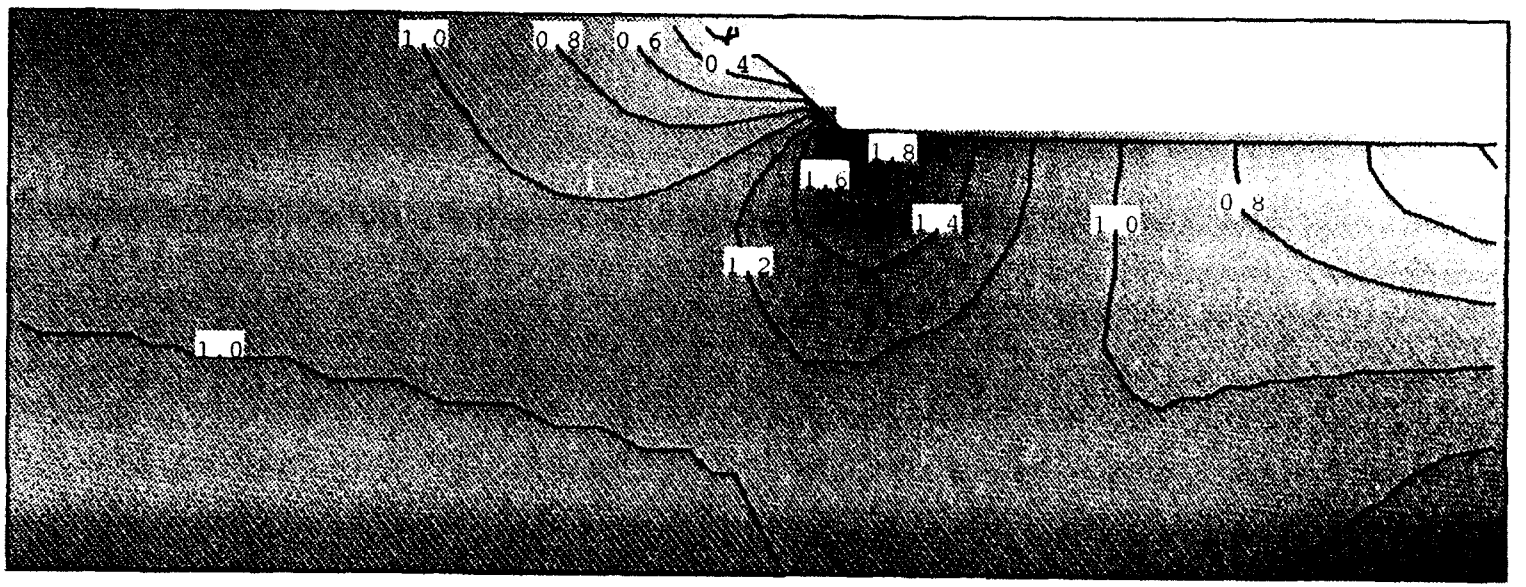

Figure 6. Dilatations due to a P wave incident at 30° from the vertical, low pass filtered with corner at 15 Hz. The dimensions of the plot are 290 m x 110 m. The amplitudes, indicated by both contour lines and grayscale intensity, are normalized to the amplitudes from a reference calculation with a flat surface and the same incident P wave. The reference amplitudes at a grid location is the amplitude at the same distance below the free surface as the location. The amplitudes can be viewed as the excitation by a dilatational source at each grid point.

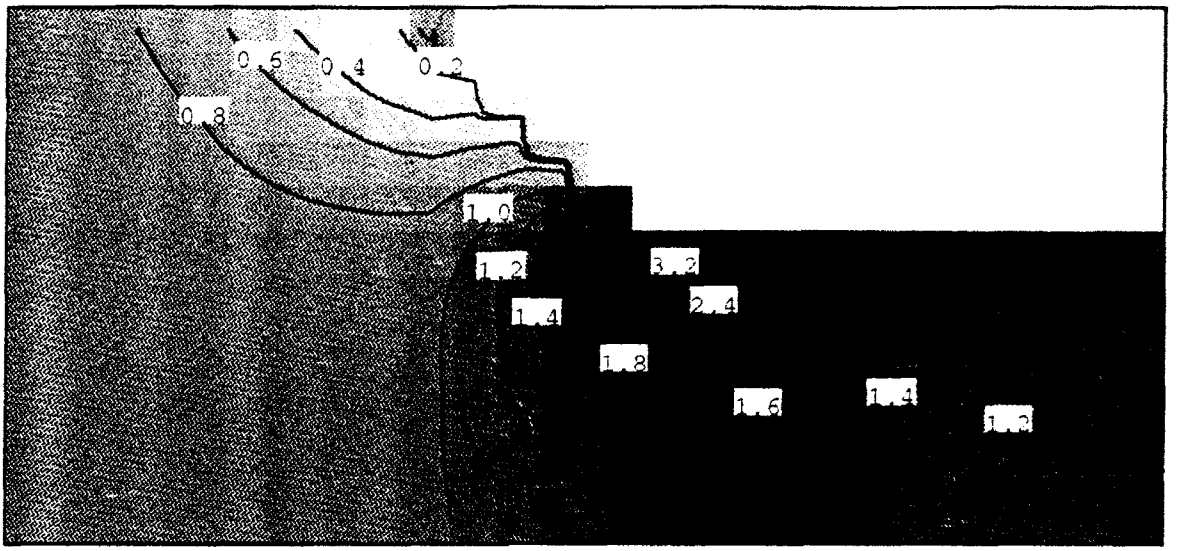

Figure 7. Exploded view of the bench from Figure 6: Dilatations due to a P wave incident at 30° from the vertical, low pass filtered with corner at 15 Hz. The dimensions of the plot are 110 m x 50 m.

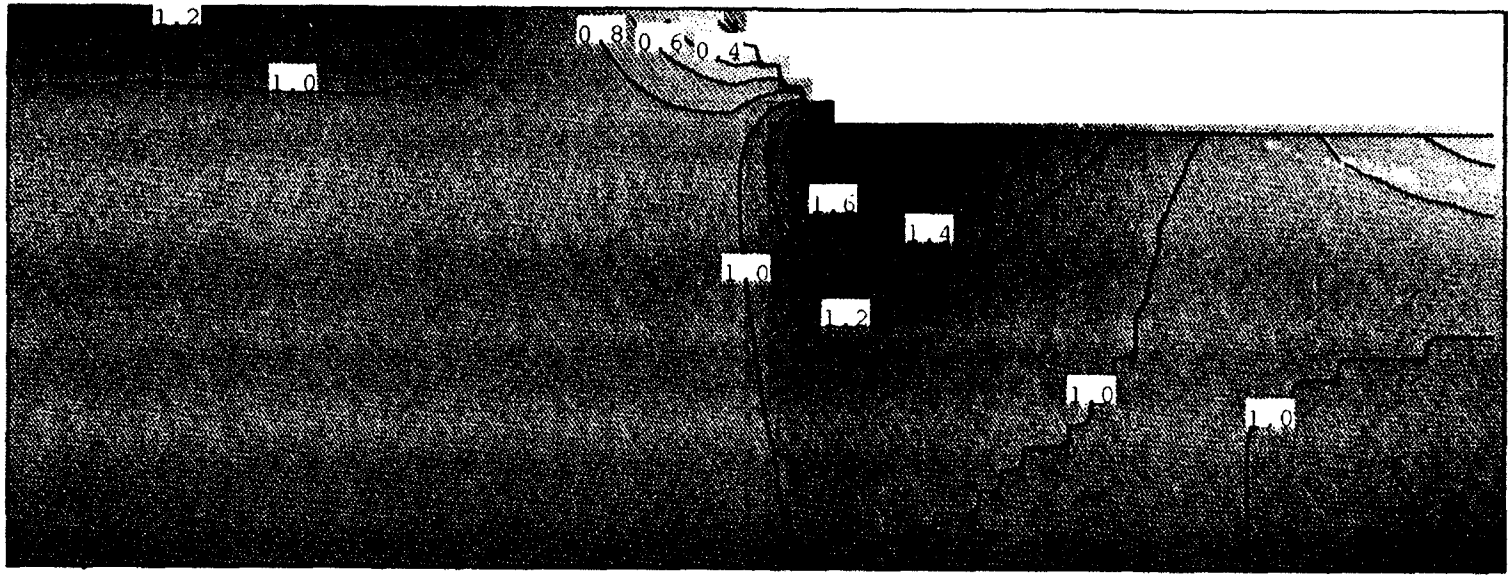

Figure 8. Dilatations due to a P wave incident at 60° from the vertical, low pass filtered with corner at 15 Hz. The dimensions of the plot are 140 m x 50 m.

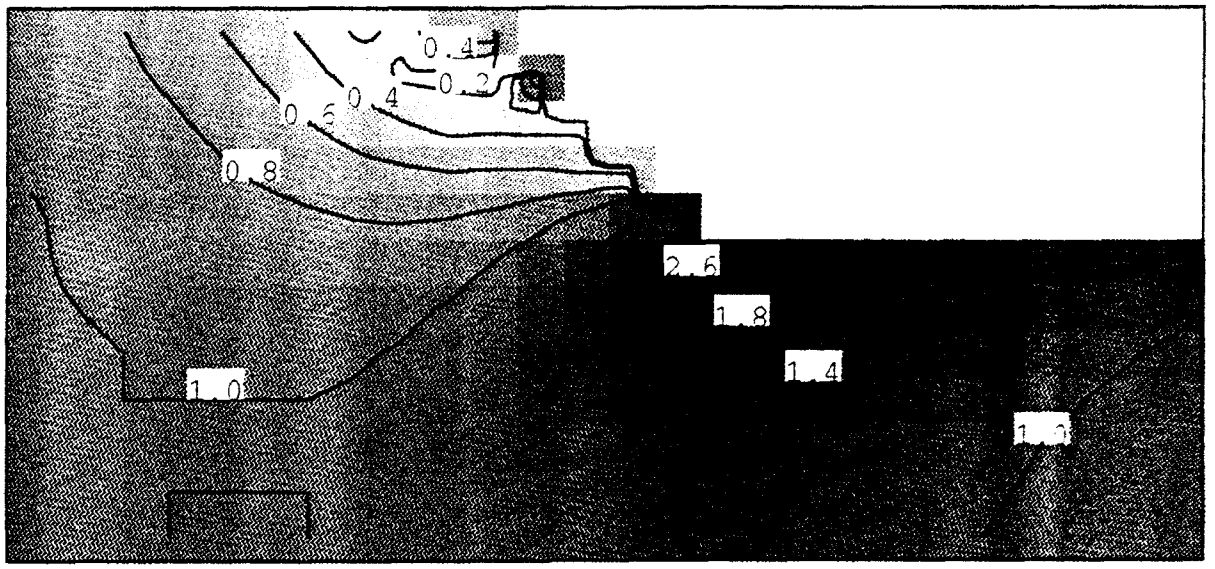

Figure 9. Exploded view of the bench showing dilatations due to a P wave incident at 30° from the vertical, low pass filtered with corner at 10 Hz. The dimensions of the plot are 100 m x 50 m.

the bench while reducing them behind it. The amplification is not relevant to interpretations of observations of standard quarry blasts since it is not usual practice to set charges on the quarry floor. However, this is a possible mechanism for increasing the amplitude of signals from quarry charges relative to a clandestine bomb.

We show in Figure 10 the dilatation field for a wave impinging from behind the bench rather than from the front, as in Figures 5 through 9. The incidence angle is 30°. In Figure 10, the excitation is diminished behind the bench, similar to Figure 7. The amplification at the floor of the bench also extends up the bench slightly.

The proximity of the bench acts to produce SV waves from an explosive source. Consider Figures 11 and 12, in which the dilatation field due to an incident SV and the rotation field due to a P wave, respectively, are shown. The incidence angle is 30° in the figures. The strains in both cases are the result of reflections at the free surface - they are zero for the incident wave. As with the dilatations in Figure 6, there is an increased apparent "source conversion" directly in front of the bench and a reduction behind the bench in both Figures 11 and 12.

SV waves excited by a deviatoric source are enhanced behind the bench, as seen in Figure 13, which displays the shear strain field due to an SV wave incident at 30°. Thus, for a source with a deviatoric component such as a compensated linear vector dipole (CLVD), the shear waves are enhanced behind the bench, while the P waves are reduced.

2.2.1 Rayleigh Waves

Figures 14 and 15 show the normalized dilatation field for Rayleigh waves experiencing a step up in topography and a step down, respectively. The monitor stations were located at the positions shown in Figure 16. Again, by reciprocity, the values on the plots can be interpreted as the relative excitation of Rayleigh waves due to dilatational sources. The Rayleigh wave amplitudes are normalized to the incoming signal at the left side of the grid. In each case, going up-step and down-step, there is a reduction of about a factor of three to five behind the bench. The effect of the step extends from the step to a distance about equal to the step

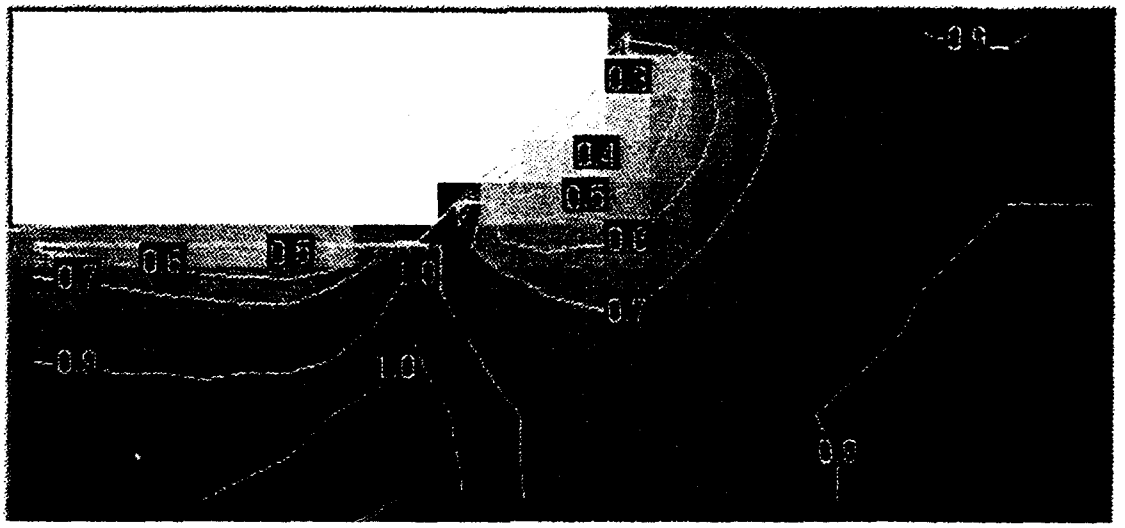

Figure 10. Exploded view of the bench showing dilatations due to a P wave incident at 30° from the vertical, low pass filtered with corner at 15 Hz (step down). The dimensions of the plot are 100 m x 50 m.

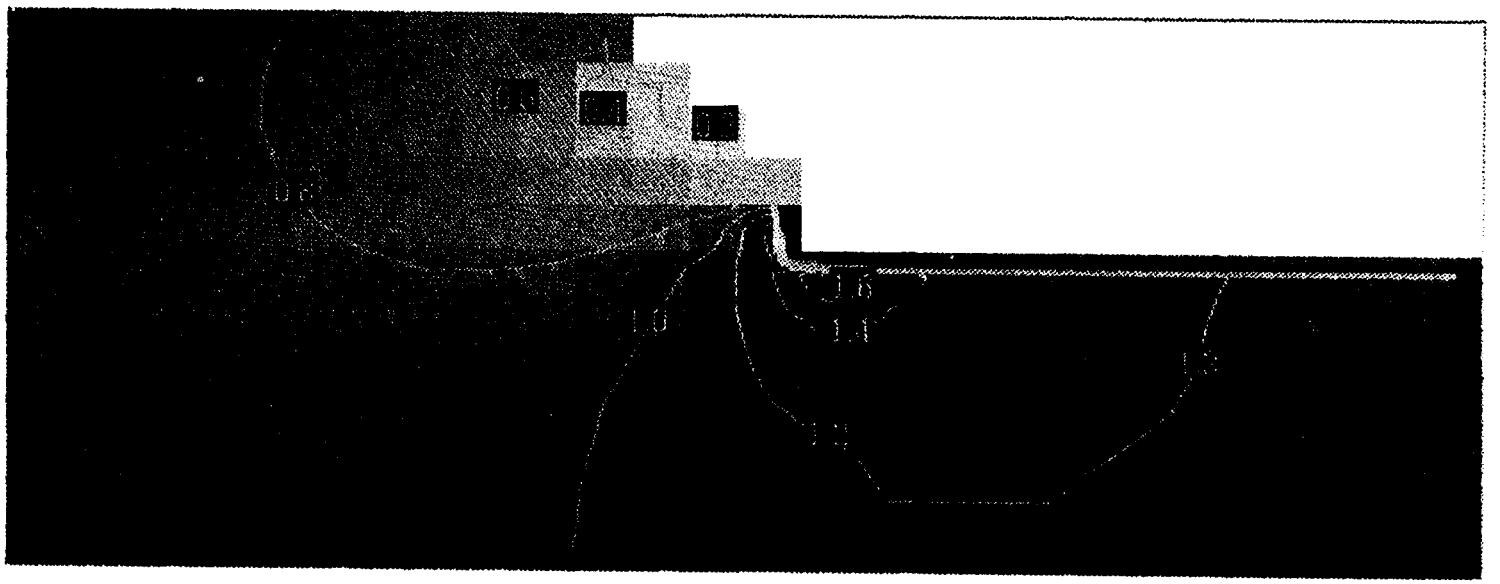

Figure 11. Exploded view of the bench showing dilatations due to an SV wave incident at 30° from the vertical, low pass filtered with corner at 15 Hz. The dimensions of the plot are 120 m x 50 m. The amplitudes can be viewed as the excitation of SV waves by a dilatational source at each grid point.

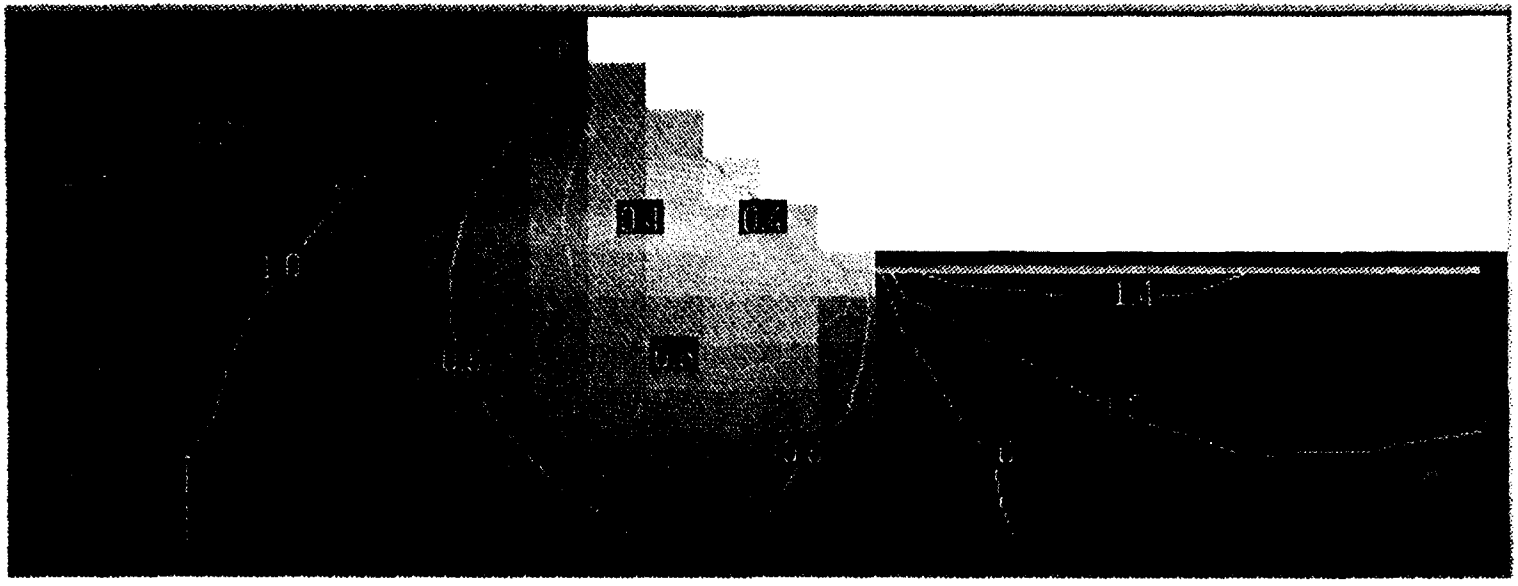

Figure 12. Exploded view of the bench showing rotations due to a P wave incident at 30° from the vertical, low pass filtered with corner at 15 Hz. The dimensions of the plot are 120 m x 50 m. The amplitudes can be viewed as the excitation of P waves by a deviatoric source at each grid point.

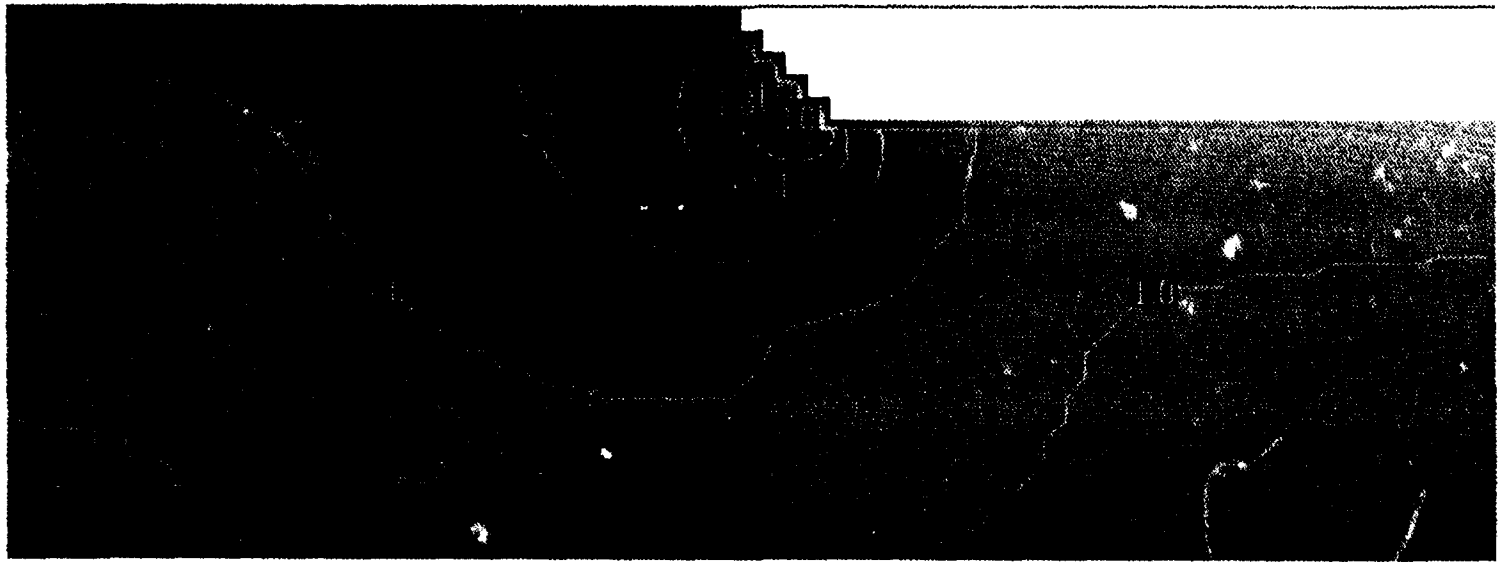

Figure 13. Rotations due to a SV wave incident at 30° from the vertical, low pass filtered with corner at 15 Hz. The dimensions of the plot are 220 m x 90 m. The amplitudes can be viewed as the excitation of SV waves by a dilatational source at each grid point.

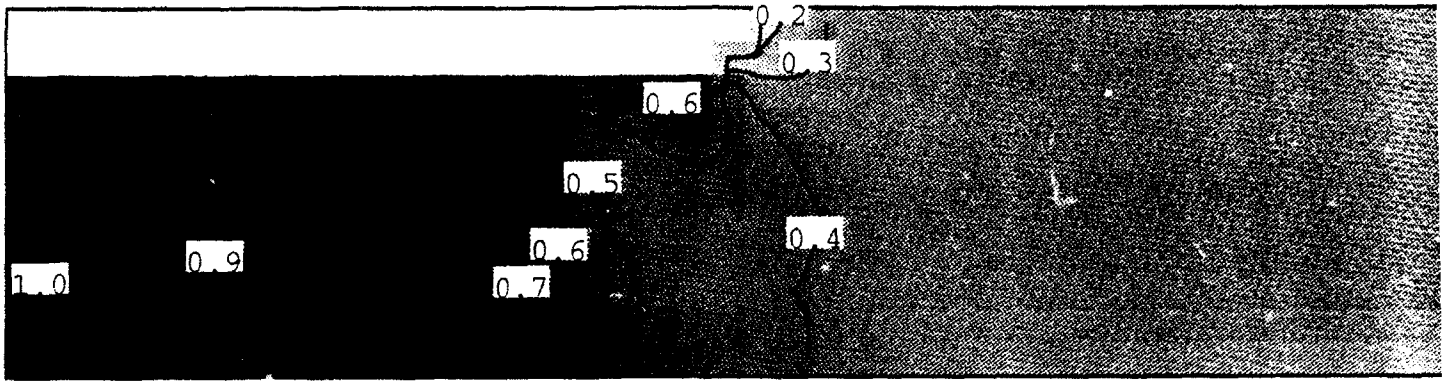

Figure 14. Normalized dilatation field for Rayleigh waves experiencing a step up in topography, low pass filtered with corner at 15 Hz. The dimensions of the plot are 330 m x 90 m. The values on the plots can be interpreted as the relative excitation of Rayleigh waves due to dilatational sources. The Rayleigh wave amplitudes are normalized to the incoming signal at the left side of the grid.

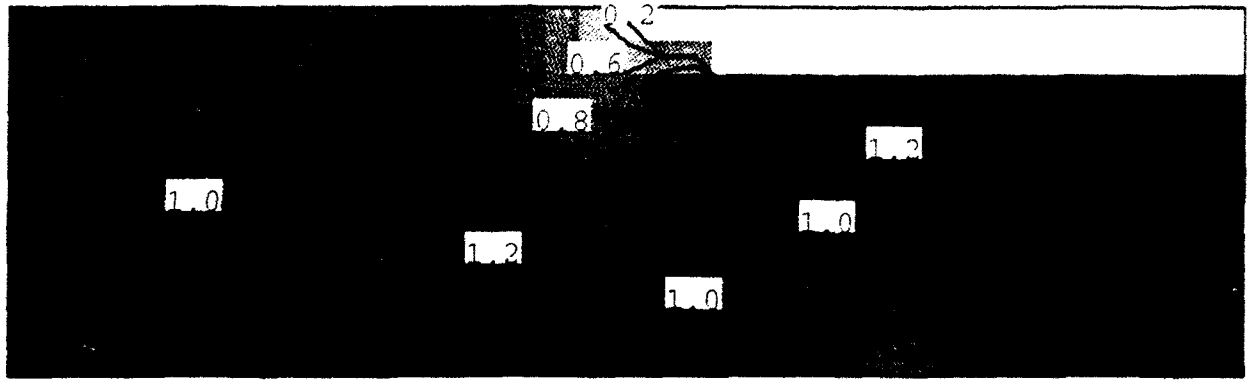

Figure 15. Normalized dilatation field for Rayleigh waves experiencing a step down in topography, low pass filtered with corner at 15 Hz. The dimensions of the plot are 290 m x 90 m. The values on the plots can be interpreted as the relative excitation of Rayleigh waves due to dilatational sources. The Rayleigh wave amplitudes are normalized to the incoming signal at the left side of the grid.

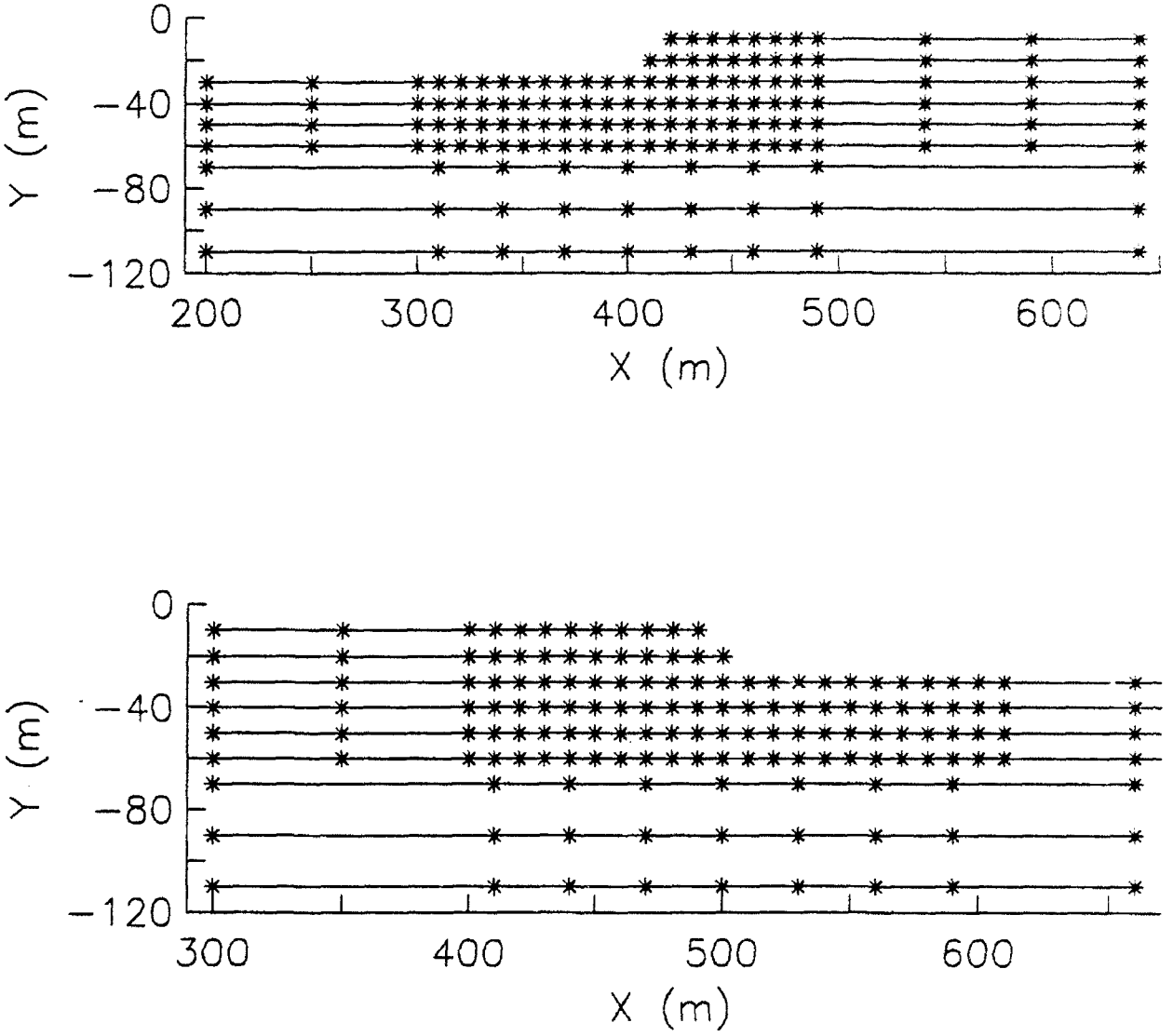

Figure 16. Locations on numerical grid at which displacements, dilatations and rotations from incident Rayleigh waves were saved for analysis: (top) step up and (bottom) step down.

height for the step-down case (Figure 15). This is true for the step-up case (Figure 14) to the left of the step, but in addition, the amplitudes are reduced to a value of 0.4 everywhere on the plot to the right of the step. In either case (step up or down), the source excitation near the bench is significantly reduced. The corresponding displacement fields are shown in Figures 17 and 18. The step-down case shows a reduction in amplitude of about 20 percent behind the step (Figure 18), while the field is uniformly reduced by a factor of 0.6 to the right of the step for the step-up case (Figure 17). Thus, Rayleigh wave amplitudes from a vertical force near the step will be slightly reduced near the step if the wave travels up-step, but will be reduced by about 40 percent anywhere behind the step if the wave travels down-step.

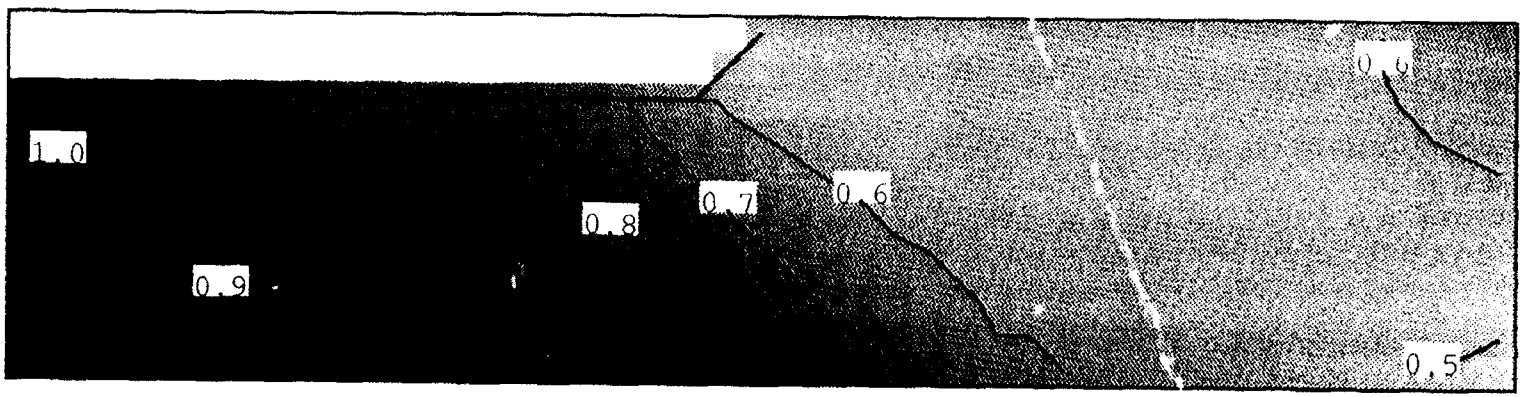

Figure 17. Normalized displacement field for Rayleigh waves experiencing a step up in topography, low pass filtered with corner at 15 Hz. The dimensions of the plot are 390 m x 90 m. The values on the plots can be interpreted as the relative excitation of Rayleigh waves due to vertical point forces. The Rayleigh wave amplitudes are normalized to the incoming signal at the left side of the grid.

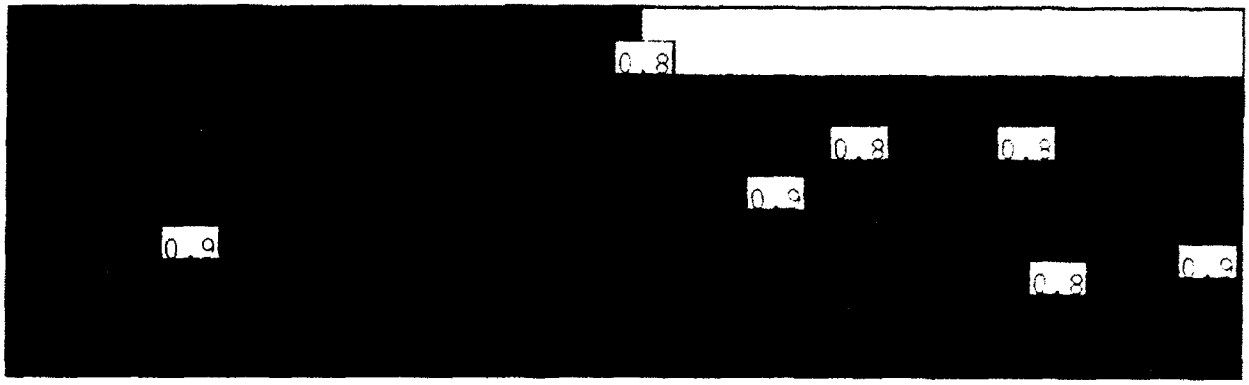

Figure 18. Normalized displacement field for Rayleigh waves experiencing a step down in topography, low pass filtered with corner at 15 Hz. The dimensions of the plot are 320 m x 90 m. The values on the plots can be interpreted as the relative excitation of Rayleigh waves due to vertical point forces. The Rayleigh wave amplitudes are normalized to the incoming signal at the left side of the grid.

3. Discussion

Recent work by Stevens, *et al.* (1993) has demonstrated that the long period seismic waves radiated by an explosion near a vertical free surface may be significantly reduced with respect to an explosion under a flat free surface. Such situations occur for explosions in a mountain or ridge. Stevens, *et al.* (1993) considered only the surface waves radiated by such structures. Here, we extend the discussion to the effects of a vertical free surface adjacent to an explosion source such as might occur in a quarry. Because of the scale of typical quarry faces (less than 30 meters) the pertinent wavelengths of phases such as P, Pg, Lg, and Rg in regional seismic waveforms are much longer than the quarry face. The same mechanism that is responsible for the reduction in surface wave excitation by an explosion in a mountain applies to the reduced excitation of regional phases by an explosion behind a vertical quarry face. Indeed, we argue that the effective moment tensor component that describes the horizontal couple perpendicular to the face of the quarry is reduced. A simple derivation for this effect is given below. The following mathematical exposition provides a theoretical framework for the interpretation of the simulations presented here and a formalism for including a source near a bench in layered media calculations. We show that for wavelengths longer than the burden of the quarry blast, we can modify the affected component of the explosion moment tensor and a halfspace Green's function may be used for seismic propagation calculations. This approximation simplifies the computation of theoretical seismograms from a quarry blast for frequencies of interest.

We are interested in the effective radiation pattern from an explosion source behind a quarry bench. The geometry is shown in Figure 19. The point explosion source is located at $\eta_1 = 0$, a distance, h, to the left of the vertical bench. h is referred to as the burden of the quarry blast. Typical quarry blast practice is to choose a burden between 30 percent and 100 percent the height of the bench.

The seismic displacement at a location, $\vec{X}$, from an explosion source with moment tensor, $M_{ij} = \delta_{ij} M_o$ at location $\vec{\eta}$ may be written as

$$U_i(\vec{X}) = \frac{M_o}{3K(\vec{\eta})} C_{kkpq}(\vec{\eta}) G_{ip,q}(\vec{X}, \vec{\eta}), \qquad (1)$$

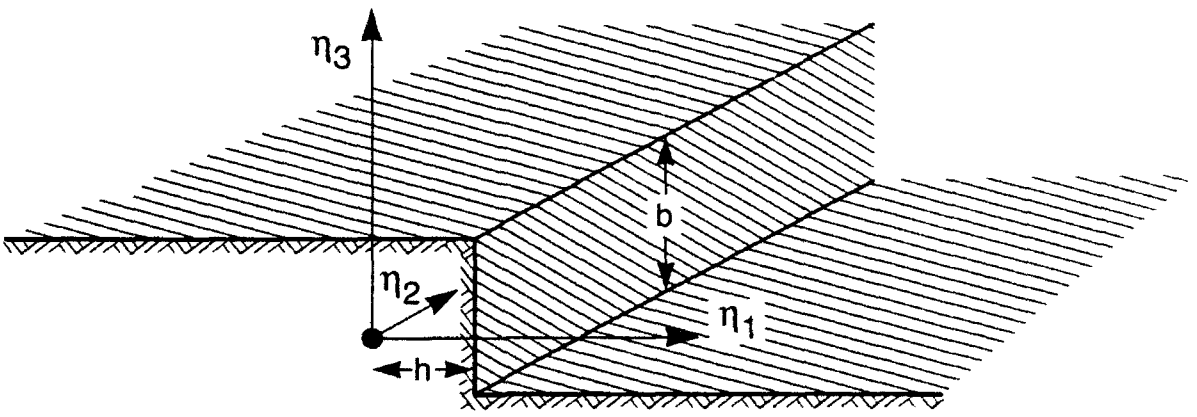

b = Bench Height
h = Burden or Source Distance to Bench Face

Figure 19. Bench geometry.

where $U_i(\vec{X})$ is the i'th component of displacement at location, $\vec{X}$, $K = \lambda + 2\mu / 3$ is the bulk modulus at the source location, $C_{ijpq}(\vec{\eta})$ is the elastic tensor, and $G_{ip,q}(\vec{X}, \vec{\eta})$ is the q'th derivative of the Green's tensor response for the i'th component of motion at $\vec{X}$ given a force in the p'th direction at location $\vec{\eta}$.

Note that by reciprocity,

$$C_{kkpq}(\vec{\eta})G_{ip,q}(\vec{X}, \vec{\eta}) = \sigma_{11}(\vec{\eta}) + \sigma_{22}(\vec{\eta}) + \sigma_{33}(\vec{\eta}), \tag{2}$$

where σ_{11}, σ_{22} and σ_{33} are stress terms at location $\vec{\eta}$ due to a displacement in the i'th direction at location $\vec{X}$. We now make use of this reciprocal problem, where σ_{ij} is the stress tensor at $\vec{\eta}$ due to a displacement at $\vec{X}$. Similarly, we will write u_j as the displacement at $\vec{\eta}$ due to a displacement at $\vec{X}$. Dependence on the location $\vec{X}$ and the i'th direction of motion is suppressed for clarity of notation in the following discussion.

Now, we know on the vertical bench (a vertical free surface) that $\sigma_{11} = 0$, and we expand the η_1 dependence of σ_{11} in a Taylor's expansion from the bench.

$$\sigma_{11}(\eta_1 = 0) = \sigma_{11}(\eta_1 = h) - h\frac{\partial \sigma_{11}}{\partial \eta_1}|_{\eta_1 = h} = -h\frac{\partial \sigma_{11}}{\partial \eta_1}|_{\eta_1 = h} \tag{3}$$

We have the equation of motion which states that

$$\frac{\partial \sigma_{11}}{\partial \eta_1}|_{\eta_1 = h} + \frac{\partial \sigma_{12}}{\partial \eta_2}|_{\eta_1 = h} + \frac{\partial \sigma_{13}}{\partial \eta_3}|_{\eta_1 = h} = \rho \ddot{u}_1(h) \tag{4}$$

together with the free surface boundary conditions on the bench (at $\eta_1 = h$)

$$\frac{\partial \sigma_{12}}{\partial \eta_2}|_{\eta_1 = h} = \frac{\partial \sigma_{13}}{\partial \eta_3}|_{\eta_1 = h} = 0 \tag{5}$$

hence we can state for the horizontal equation of motion on the bench

$$\frac{\partial \sigma_{11}}{\partial \eta_1}|_{\eta_1 = h} = \rho \ddot{u}_1(\eta_1 = h) \tag{6}$$

Therefore,

$$\sigma_{11}(\eta_1 = 0) = -h\,\rho\,\ddot{u}_1(\eta_1 = h) \tag{7}$$

We approximate $\ddot{u}_1(\eta_1 = h)$ by the halfspace solution, $\ddot{u}_1^{(HS)}(\eta_1 = h)$, and we can write

$$\sigma_{11}(\eta_1 = 0) \approx -h\,\rho\,\ddot{u}_1^{(HS)}(\eta_1 = h)\,. \tag{8}$$

This says that the σ_{11} stress from a displacement source at location $\bar{X}$ is proportional to the distance from the bench, h, and density, ρ.

How much is the explosion behind a bench reduced with respect to an explosion in a halfspace? We can estimate this effect by writing the expression for the halfspace σ_{11} component of stress in terms of the halfspace displacements,

$$\sigma_{11}^{(HS)} = (\lambda + 2\mu)\frac{\partial u_1^{(HS)}}{\partial \eta_1} + \lambda\left(\frac{\partial u_2^{(HS)}}{\partial \eta_2} + \frac{\partial u3^{(HS)}}{\partial \eta_3}\right). \tag{9}$$

To estimate the ratio $\Gamma = \dfrac{\sigma_{11}}{\sigma_{11}^{(HS)}}$ we neglect the second term to get

$$\sigma_{11}^{(HS)} \approx \rho\,\alpha^2\,\frac{\partial u_1^{(HS)}}{\partial \eta_1}\,. \tag{10}$$

We note that for plane P waves propagating in the η_1 direction we can make the approximation that

$$\left|\frac{\partial u_1^{(HS)}}{\partial \eta_1}\right| \approx \frac{\omega}{\alpha}\left|u_1^{(HS)}\right| \tag{11}$$

so we have that

$$\Gamma = \frac{\sigma_{11}}{\sigma_{11}^{(HS)}} \approx \frac{\rho h \omega^2 u_1^{(HS)}}{\rho\alpha\omega u_1^{(HS)}} = \frac{\omega h}{\alpha} = kh\,. \tag{12}$$

For, h = 10 m, α = 2000 m/s, we have Γ(10Hz) = 0.31, Γ(5Hz) = 0.15, and Γ(1Hz) = 0.031. This would indicate that the P-waves radiated perpendicular to the bench

will be substantially reduced with respect to the halfspace for much of the bandwidth of regional seismograms.

However, it is clear that the radiation pattern from an explosion behind the quarry bench will depend upon the slowness and the azimuth of the radiated wave. That is to say that $\Gamma = \Gamma(\vec{k},h)$. A complete treatment of this problem therefore requires the solution of the complete scattering problem using numerical techniques as in the previous section.

To summarize, for kh << 1 the M_{11} component of an explosion behind the bench can be modified and halfspace Green's functions can be used to propagate the seismic waves. To formalize this, we re-write Equation (1) as,

$$U_i(\vec{X}) = \frac{M_o}{3K}\Big(\Gamma_{11}(\vec{k},h)C_{kk11}\,G_{i1,1}^{(HS)}(\vec{X},\eta) + \Gamma_{22}(\vec{k},h)C_{kk22}\,G_{i2,2}^{(HS)}(\vec{X},\eta) + \Gamma_{33}(\vec{k},h)C_{kk33}\,G_{i3,3}^{(HS)}(\vec{X},\eta)\Big) \quad . \tag{13}$$

For kh << 1, we have argued that $\Gamma_{11}(\vec{k},h) \approx kh << 1$, while $\Gamma_{22}(\vec{k},h) \approx 1$ and $\Gamma_{33}(\vec{k},h) \approx 1$. And we approximate Equation (13) by,

$$U_i(\vec{X}) \approx \frac{M_o}{3K}\Big(kh\,C_{kk11}\,G_{i1,1}^{(HS)}(\vec{X},\eta) + C_{kk22}\,G_{i2,2}^{(HS)}(\vec{X},\eta) + C_{kk33}\,G_{i3,3}^{(HS)}(\vec{X},\eta)\Big) \tag{14}$$

which may be more simply written for an isotropic medium,

$$U_i(\vec{X}) \approx M_o\Big(kh\,G_{i1,1}^{(HS)}(\vec{X},\eta) + G_{i2,2}^{(HS)}(\vec{X},\eta) + G_{i3,3}^{(HS)}(\vec{X},\eta)\Big) \quad . \tag{15}$$

It should be readily apparent from this expression that the radiated seismic waves will have an azimuthal radiation pattern and the source will radiate S H waves.

4. Conclusions

We have computed the strain and displacement fields due to plane waves incident on a uniform solid with a topographic bench at the surface. Using the reciprocity arguments discussed above, this allows us to map the relative excitation of waves due to point dilatational and force sources at and near the bench. We find that the excitation of waves on the bench where quarry blasting would occur are influenced relative to the excitation of waves in a flat half-space, in the following ways.

1. Seismic signals from point explosion (dilatational) sources located behind the quarry face can be reduced substantially in amplitude, while seismic waves from sources on the quarry floor may be amplified. The source amplitude variations occur for sources within about one bench height of the quarry face. The numerical simulations presented in this study can be used to estimate and correct for this effect.

2. An extended source in the standard configuration (charges placed a distance of 1/2 the bench height from the quarry face and extending to the depth of the quarry floor) averages these variations leading to a source that is reduced slightly in amplitude relative to a source in a half space.

3. The amplitude variations occur because a dilatational source such as an explosion is strongly affected by the presence of a free surface close to the source. Seismic signals from point forces are affected very little by proximity to the quarry face.

4. These results are nearly independent of the takeoff angle of the seismic signal.

5. Rayleigh wave amplitudes are reduced by up to 40 percent.

In terms of modeling quarry blast ground motions, such as in Barker, *et al.* (1993), this study suggests that when computing regional phases such as Pn, Pg, Lg using plane layered models, the M_{11} component from the explosive charges should be reduced by a factor of 2 or 3 while the forces from the spall phases need not be scaled. The contributions to regional phases from spall were found in Barker, *et al.* (1993) to be comparable to those from the explosive charges. The

results here argue that the explosive component of the blast be reduced up to a level about 50 percent that of the spall component. Therefore, in the far-field, for wavelengths longer then the quarry bench height, the spall components of a quarry blast are expected to exceed the explosive part of the quarry blast for wave radiated perpendicular to the quarry bench.

Furthermore, the apparent reduction of M_{11} relative to M_{22} and M_{33} implies an apparent deviatoric source that will radiate SH waves from an explosion behind the bench. The enhanced SH and SV radiation contribute to the Lg excitation by quarry blasts relative to normally buried and overburied explosions that are not adjacent to vertical free-surfaces such as a quarry face.

5. References

Aki, K. and P.G. Richards (1980), "Quantitative Seismology," W.H. Freeman and Company, San Francisco.

Barker, T.G. K.L. McLaughlin and J.L. Stevens (1993), "Numerical Simulation of Quarry Blast Sources," S-CUBED Technical Report to DARPA, SSS-TR-93-13859.

Jih, R.-S., K.L. McLaughlin and Z.A. Der (1988), "Free-boundary Conditions of Arbitrary Polygonal Topography in a Two-Dimensional Explicit Elastic Finite-Difference Scheme," *Geophysics, 53(8)*, pp 1405-1055.

McLaughlin, K.L. and R.-S.Jih (1988), "Scattering from near-Source Topography: Teleseismic Observations and Numerical Simulations," *Bull. Seism. Soc. Am., 78(4)*, pp 1399-1414.

McLaughlin, K.L. and L.M. Anderson (1987), "Stochastic Dispersion of Short-Period P-Waves Due to Scattering and Multipathing," *Geophys. J. R. astr. Soc., 89*, pp 833-963.

Okamoto, T. (1993), "The Effects of Sedimentary Structure and Bathymetry near the Source on Teleseismic I Waveforms from Shallow Subduction Zone Earthquakes," *Geophys. J. Int., 112*, pp 471-480.

Sheriff, R.E. and L.P. Geldart (1982), "Exploration Seismology: History, Theory, and Data Acquisition," Cambridge University Press.

Stevens, J. L., K. L. McLaughlin, B. Shkoller, and S. M. Day (1992). "Two-Dimensional Axisymmetric Calculations of Surface Waves Generated by an Explosion in an Island, Mountain and Sedimentary Basin," *Geophys. J. Int.*, in press.